One-pot synthesis of pyrazole conjugated tetrahydroquinolines using [DBUH][OAc] and assessment of their anti-cancer activity

Kulkarni Kalpana[a] and V. Anitha Rani[b]

[a]*Department of Humanities and Sciences (Chemistry), Gokaraju Rangaraju Institute of Engineering and Technology, Bachupally, Hyderabad- 500 090, India.*

[b]*Department of Chemistry, Institute of Aeronautical Engineering, Dundigal, Hyderabad-500043, India*

Corresponding author: kalpanakulkarni26@gmail.com ; kalpanakulkarni568@gmail.com

Abstract--The pyrazole scaffold is a key component of many medicinally active novel chemical substances. Treatment of 3-methyl-1-phenyl-1H-pyrazol-5-amine **1**, 5,5-dimethylcyclohexane-1,3-dione **2**, and benzaldehydes **3** with [DBUH][OAc] as green reaction medium at 70-75^{o}C for 40-60 min formed pyrazole conjugated tetrahydroquinoline derivatives **4** with 85-90 % yield. Further, the synthesized compounds were evaluated for their cytotoxic potential against SKOV-3 and PC-3 cells. Compound 4g and 4d showed good anticancer activity against both the cell lines with IC_{50} values ranges from 8.1 to 10.2 µM. Later, the active compounds 4g and 4d examined for molecular binding studies towards Human Phosphodiesterase 4B protein. Compound 4g showed good binding affinity such as 8.5 Kcal/mol against target protein.

Keywords: [DBUH][OAc], Environmentally benign synthesis 3-methyl-1-phenyl-1H-pyrazol-5-amine, 5,5-dimethylcyclohexane-1,3-dione, and one-pot reaction.

INTRODUCTION

The pharmacological activity of pyrazolo[3,4-b]quinoline derivatives were significant. They displayed anticancer, antimalarial, antiviral, and anti-inflammatory activities in particular [1-3]. These were also found to have parasiticidal, antibacterial, anticancer, hypotensive, and vasodilatory properties. A particularly important representative of the condensed pyrazoles is Sildenafil (Viagra®). It inhibits the phosphodiesterase-5 and thus enables the amplification of the relaxing effect of nitric oxide a natural erection reaction on sexual stimulus. It can also be used to treat a pulmonary hypertension. Riociguat is a vasodilating drugs, the stimulators of soluble guanylate cyclase. Zaleplon has a pyrazolopyrimidine system and belongs to non-benzodiazepine-like hypnotics (Sleeping pills). Like the benzodiazepines, it acts on the GABAA receptor chloride

channel. Two pyrazole pregnanes Cortisuzol and Cortivazol of the condensed pyrazoles are anti-inflammatory and anti-allergic acting glucocorticoids, respectively. Stanozolol is a steroid anabolic that is effective orally and compared to Methyltestosterone has a 10-fold stronger musculotropic effect [4].

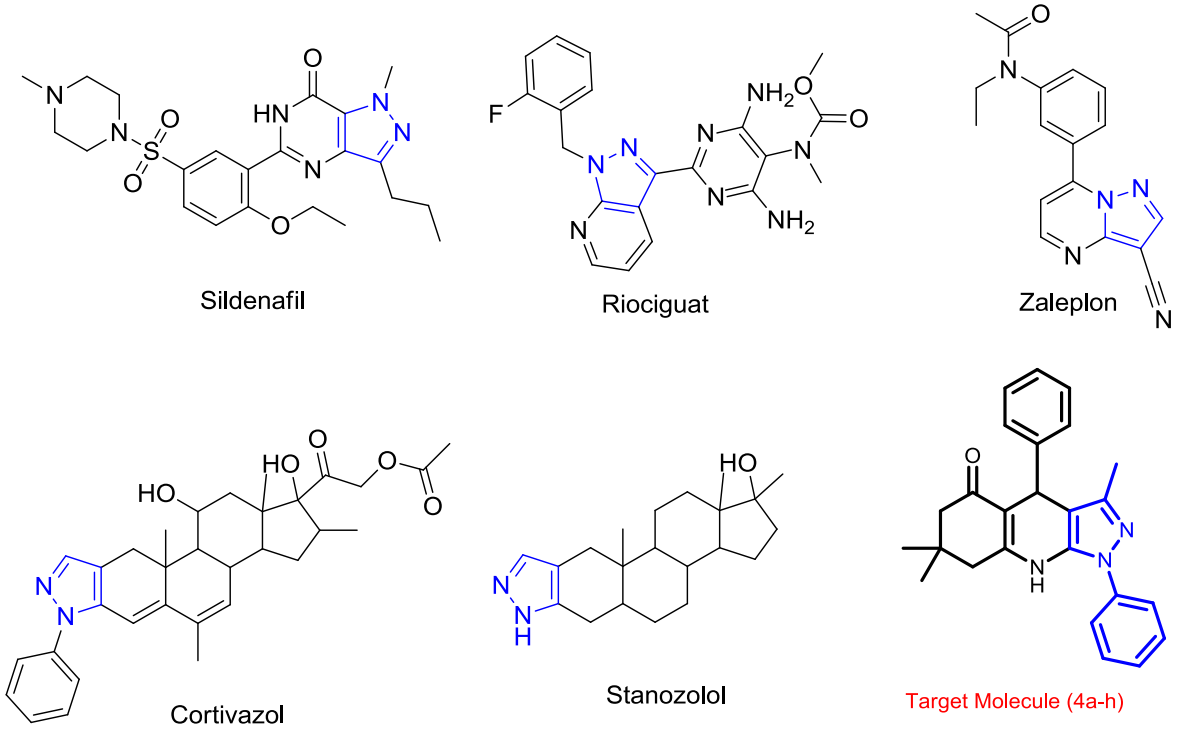

Figure 1: Pyrazole scaffold containing therapeutically active drugs

Various synthetic procedures for the creation of pyrazolo-[3,4-b]-quinoline scaffolds employing diverse homogeneous and heterogeneous materials such as FeNi3-ILs [5], $PEGOSO_3H$[6], L-proline [7], and $InCl_3$[8] as catalysts have been published in the recent past due to their expanding relevance. Long reaction durations, harsh reaction conditions, catalyst separation issues, arduous workup, waste production, toxic solvents, high reaction temperatures, and low product yields are all disadvantages of the aforementioned processes. As a result, there is a pressing need for fresh approaches that can overcome the aforementioned obstacles.

The study for alternative reaction media that can replace the dangerous, poisonous and combustible organic solvents that represent such a major environmental concern is progressing. For numerous organic processes, ecologically friendly reaction media such as green solvents [9], ionic liquids[10], supercritical fluids [11], and fluorous phases [12] are utilized. Each has its own set of benefits and is influenced by elements such as lipophilicity, pressure, and viscosity.

In consideration of the significance of the pyrazole scaffold, we present a simple one-pot method for the synthesis of pyrazolo-[3,4-b]-quinolines that uses [DBUH][OAc] as the green reaction medium.

Results and Discussion:

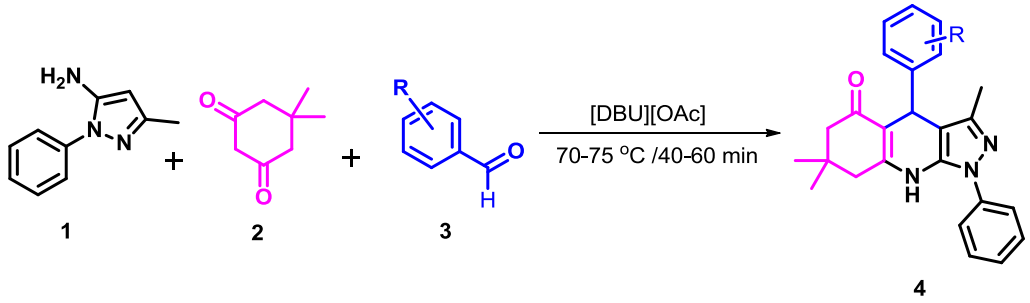

SCHEME 1: Synthesis of 4a-4h by one-pot synthesis.

At first, a one-pot three-component reaction of 3-methyl-1-phenyl-1H-pyrazol-5-amine **1** (1 mmol) with 5,5-dimethylcyclohexane-1,3-dione **2** (1 mmol) and benzaldehydes **3a** (1 mmol) was carried out at 70-75 ^{o}C as a model for the synthesis of 3,7,7-trimethyl-1,4-diphenyl-6,7,8,9-tetrahydro-1H-pyrazolo[3,4-b]quinolin-5(4H)-one **4a**, Table-1 presents a summary of the findings. The best results were obtained when [DBUH][OAc] (6 eq) was used as an ionic liquid at 70-75 ^{o}C for 40-60 minutes to generate the title chemical with a 90% yield. ^{1}H-NMR, IR, and Mass spectroscopy were used to characterise and confirm the structure of chemical **4a.**

The model reaction was next investigated with regard to 3-methyl-1-phenyl-1H-pyrazol-5-amine **1** in the presence of varying amounts of ionic liquid [DBUH][OAc] (3 eq, 6 eq, and 9 eq). However, the one-pot reaction of 1 (1 eq), 2 (1 eq), and 3 (1 eq) for 90 minutes at 70-75 ^{o}C in the presence of [DBUH][OAc] as a reaction medium (6 eq) yielded the best yield (90%) **(Table 1, entry 6).**

Entry	Ionic liquid/6 eq	Temperature(^{o}C)	Time (min)	4a (%)
1	[bmim][Br]	45-50	600	81
2	[bmim][OH]	45-50	400	80
3	[DBUH][OAc]	45-50	200	82
4	[bmim][Br]	45-50	90	84
5	[bmim][OH]	70-75	50	81
6	**[DBUH][OAc]**	**70-75**	**40**	**90**

7	[bmim][Br]	85-90	80	83
8	[bmim][OH]	85-90	50	82
9	[DBUH][OAc]	85-90	30	82

Table 1: Effect of Ionic liquid (6 eq) and temperature on one-pot reaction of **1**, **2 & 3a** to from **4a.**

Entry	Ionic liquid	Quantity (eq)	Time (min)	5a (%)
1	[DBUH][OAc]	3 eq	90	82
2	**[DBUH][OAc]**	**6 eq**	**40**	**90**
3	[DBUH][OAc]	9 eq	35	84

Table 2: Quantity of Ionic liquid at 70-75 ^{o}C on one-pot four component reaction of **1**, **2, & 3a** to from **4a.**

We investigated the breadth and limits of a series of substituted anilines **3a-3h** after optimising one-pot three component reaction conditions. Both electron-deficient and electron-rich anilines were found to be suitable for this optimised condition, yielding pyrazole conjugated tetrahydroquinoline derivatives **4** with yields of 85-90%.

The synthesis of **4a-4h** was carried out in a one-pot three component reaction using **1**, **2** and **3a-3h** in [DBUH][OAc] as green reaction medium at 70-75^{o}C for 40-60 min, yielding pyrazole conjugated tetrahydroquinoline derivatives **4** with 85-90 % yield. ^{1}H and ^{13}C NMR, as well as mass spectroscopy, were used to confirm the structures.

Anticancer activity:

A total of 8 different analogues of pyrazole conjugated tetrahydroquinolines were synthesized and evaluated for their cytotoxic potential towards two different human cancerous cell lines such as SKOV-3 and PC-3. The compounds exhibited good to moderate activity against the examined cell lines (Table 3). Among the synthesized, compound 4g is the most active compound towards SKOV-3 and PC-3 cells with an IC_{50} values of 8.1 and 9.3 µM, respectively. In addition, the compound 4d is also showed good activity against SKOV-3 and PC-3 cells with IC50 values of 8.6 and 10.2 µM, respectively. In contrast, compound 4a did not exhibit any activity against the tested cell lines.

Test compound	IC_{50} value in µM (Mean ± S.D)	
	SKOV-3	**PC-3**
4a	>100	>100
4b	12.4 ± 0.22	13.1 ± 0.16
4c	74.6 ± 0.38	79.5 ± 0.48
4d	8.6 ± 0.12	10.2 ± 0.25
4e	11.3 ± 0.16	12.6 ± 0.21
4f	25.2 ± 0.28	19.8 ± 0.22
4g	8.1 ± 0.11	9.3 ± 0.16
4h	22.7 ± 0.32	20.9 ± 0.19
Doxorubicin	0.65 ± 0.07	0.83 ± 0.06

Table 3: Anticancer results of the synthesized compounds against human ovarian cancer cells (SKOV-3) and human prostate cancer cells (PC-3) and. All the experiments were performed in triplicates and the results are expressed as Mean ± S.D, (*n*=3).

Molecular Docking

Based on preliminary cytotoxicity results, the active compounds (4d and 4g) were further examined for their insilico binding with the target protein Human Phosphodiesterase 4B. The results demonstrated that the active molecules were bound to the active site of target protein through hydrophobic and hydrogen bond interactions. A total of ten different conformations were examined for each ligand and the best pose was presented in the Figure 2. The docked ligands 4d and 4g showed good binding energies with the target protein. As compared to 4d, 4g exhibited greater binding energy with target protein. The binding energy was found to be -8.5 kcal/mol and -8.3 kcal/mol for compound 4g and 4d, respectively. Further, the docking results are validated with re-docking of co-crystal ligand 7DE. The co-crystal ligand 7DE exhibited -9.1 kcal/mol binding energy. Both compound 4d and 4g formed one hydrogen bond with the target protein. Collected hydrogen and hydrophobic interactions were influenced the binding affinity of target protein with docked ligands Table 4.

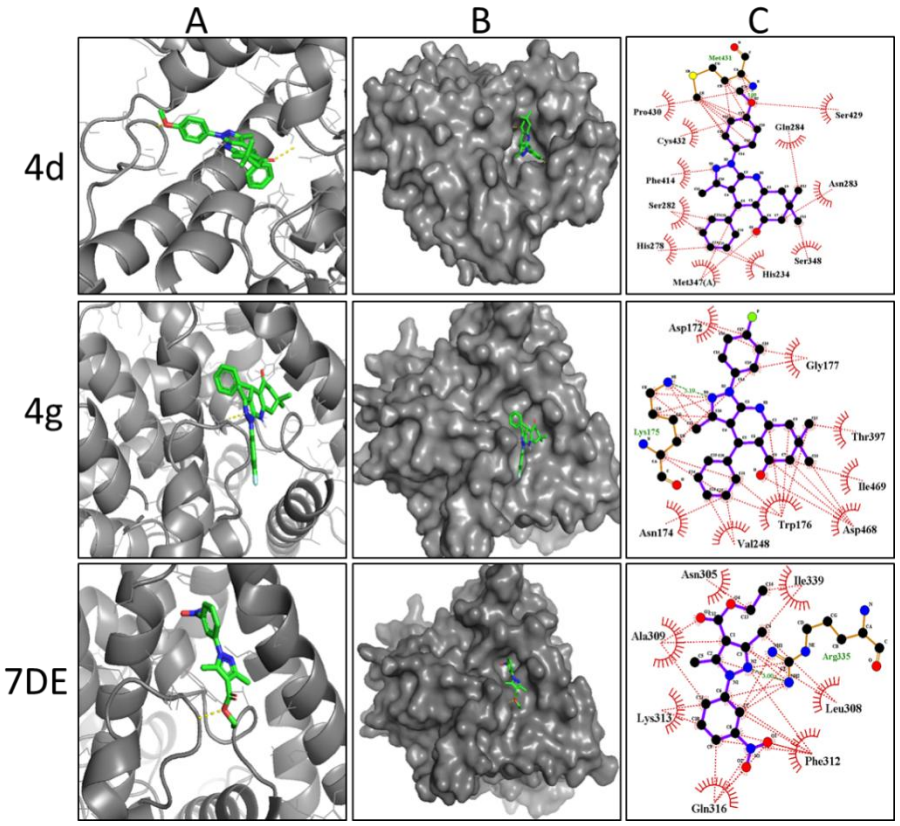

Figure 2: Insilico binding interactions of the test compounds (4d & 4g) in the active site of Human Phosphodiesterase 4B (PDB ID: 1Y2J). Among different docked conformations, the best pose for active compounds 4d and 4g was showed in the image. The co-crystal ligand 7DE was used for the validation of results.

Ligand	Binding energy (Kcal/mol)	H-bond/s	Protein–Ligand interactions
4d	-8.3	Met431	His234, His278, Ser282, Asn283, Gln284, Met347, Ser348, Phe414, Ser429, Pro430, Cys432, Asp172, Asn174, Trp176, Gly177, Val248, Thr397, Asp468, Ile469
4g	-8.5	Lys175	
7DE (Co-crystal ligand)	-9.1	Arg335	Asn305, Leu308, Ala309, Phe312, Lys313, Gln316, Ile339

Table 4: Binding energies and amino acid residues of the target protein that are interacted with docked ligands.

EXPERIMENTAL SECTION

Melting points are determined on in open capillary tubes in sulphuric acid bath. FT-IR spectra are recorded on a VERTEX 70 Brucker by using KBr. A Bruker DRX-400 spectrometer 400 and 100 MHz was employed for recording 1H NMR and 13C NMR spectra respectively and DMSO-d6 was used as solvent and TMS as an internal standard. . Mass spectra were recorded on Agilent-LCMS instrument.

GENERAL PROCEDURE:

In a typical experiment, a 50 ml round bottomed flask was charged the combination of 3-methyl-1-phenyl-1H-pyrazol-5-amine **1** (1 mmol) with 5,5-dimethylcyclohexane-1,3-dione **2** (1 mmol) and benzaldehydes **3a-3h** (1 mmol) in 6 eq of [DBUH][OAc] were charged in a 50 ml round bottomed flask and the mixture was stirred at 70-75 ^{o}C. The reaction was complete within 40-60 min as analyzed by TLC using petroleum ether/ethyl acetate (60:40) as eluent. After allowing the reaction mixture to cool to room temperature (25-30 ^{o}C), 50 mL of water was added. By filtering and washing with water and ethanol, 90 % of pure 3,7,7-trimethyl-1,4-diphenyl-6,7,8,9-tetrahydro-1H-pyrazolo[3,4-b]quinolin-5(4H)-one derivatives were obtained, as determined by spectrum data.

3,7,7-trimethyl-1,4-diphenyl-6,7,8,9-tetrahydro-1H-pyrazolo[3,4-b]quinolin-5(4H)-one (4a)

Melting Range: 191-193 ^{o}C; Yield %: 90%; ^{1}H NMR (400 MHz; DMSO-d_6;TMS) δ_H: 1.0 (s, 3H, CH_3), 1.05 (s, 3H, CH_3), 2.0 (s, 3H, CH_3), 2.2-2.4 (d, 4H, CH_2), 5.1 (s, 1H, CH), 6.5 (s, 1H, NH),7.0-8.0 (m, 10H, Ar-H); ^{13}C NMR δ_C (100 MHz; DMSO-d_6): 12.1, 27.4, 28.3, 29.6, 32.1, 36.1, 41.2, 48.7, 50.7, 104.7, 112.7, 121.5, 125.1, 126.4, 127.3, 127.6, 128.1, 129.2, 135.2, 145.9, 147.9, 195.0 ; $M^{+.1}$ = 384.

3,7,7-trimethyl-4-phenyl-1-(p-tolyl)-6,7,8,9-tetrahydro-1H-pyrazolo[3,4-b]quinolin-5(4H)-one (4b)

Melting Range: >220 ^{o}C; Yield %: 88%; MP: >220 ^{o}C; ^{1}H NMR (400 MHz; DMSO-d_6;TMS) δ_H: 0.9 (s, 3H, CH_3), 1.0 (s, 3H, CH_3), 1.7 (s, 3H, CH_3), 1.9-2.1 (d, 4H, CH_2), 5.1 (s, 1H, CH), 7.0-8.0 (m, 9H, Ar-H), 9.2 (s, 1H, NH),; ^{13}C NMR δ_C (100 MHz; DMSO-d_6): 11.8, 19.2, 26.8, 28.9, 29.0, 29.5, 40.6, 50.8, 104.8, 110.6, 120.9, 123.8, 125.5, 125.8, 126.6, 128.8, 129.5, 129.2, 134.5, 136.2, 138.4, 148.0, 148.2, 151.6, 193.8; $M^{+.1}$ = 398.

3,7,7-trimethyl-4-phenyl-1-(o-tolyl)-6,7,8,9-tetrahydro-1H-pyrazolo[3,4-b]quinolin-5(4H)-one (4c)

Melting Range: 200-202 ^{o}C; Yield %: 85%; ^{1}H NMR (400 MHz; DMSO-d_6;TMS) δ_H: 0.9 (s, 3H, CH_3), 1.0 (s, 3H, CH_3), 1.7 (s, 3H, CH_3), 1.9-2.2 (d, 4H, CH_2), 5.1 (s, 1H, CH), 7.0-8.0 (m, 9H, Ar-H), 9.3 (s, 1H, NH); ^{13}C NMR δC (100 MHz; DMSO-d_6): 11.9, 19.3, 26.9, 28.8, 31.2, 40.6, 50.8, 104.6, 110.0, 120.9, 123.5, 125.2, 125.9, 126.7, 128.9, 129.1, 129.3, 134.2, 136.3, 138.5, 145.3, 151.5, 194.2; $M^{+.1}$ = 398.

1-(4-methoxyphenyl)-3,7,7-trimethyl-4-phenyl-6,7,8,9-tetrahydro-1H-pyrazolo[3,4-b]quinolin-5(4H)-one (4d)

Melting Range: >220 ^{o}C; Yield %: 87%; ^{1}H NMR (400 MHz; DMSO-d_6;TMS) δ_H: 0.9 (s, 3H, CH_3), 1.0 (s, 3H, CH_3), 1.8 (s, 3H, CH_3), 1.8-2.0 (d, 4H, CH_2), 3.6 (s, 3H, OCH_3), 5.0 (s, 1H, CH), 7.0-8.0 (m, 9H, Ar-H), 9.2 (s, 1H, NH),; ^{13}C NMR δC (100 MHz; DMSO-d6): 11.8, 26.8, 27.5, 28.7, 31.3, 34.2, 47.2, 50.1, 54.3, 104.5, 110.2, 113.1, 120.3, 123.2, 126.1, 126.8, 128.6, 129.5, 129.9, 130.2, 136.1, 138.2, 139.4, 145.2, 151.4, 156.6, 194.5; $M^{+.1}$ = 414.

1-(2-methoxyphenyl)-3,7,7-trimethyl-4-phenyl-6,7,8,9-tetrahydro-1H-pyrazolo[3,4-b]quinolin-5(4H)-one (4e)

Melting Range: >220 ^{o}C; Yield %: 90%;^{1}H NMR (400 MHz; DMSO-d_6;TMS) δ_H: 0.9 (s, 3H, CH_3), 1.0 (s, 3H, CH_3), 1.7 (s, 3H, CH_3), 1.8-2.0 (d, 4H, CH_2), 3.6 (s, 3H, OCH_3), 4.9 (s, 1H, CH), 7.0-8.0 (m, 9H, Ar-H), 9.3 (s, 1H, NH),; ^{13}C NMR δ_C (100 MHz; DMSO-d6): 11.9, 26.9, 27.7, 28.8, 31.8, 34.4, 47.6, 50.4, 54.8, 104.6, 110.0, 113.2, 120.5, 123.5, 126.2, 126.9, 128.7, 129.8, 129.9, 130.3, 136.2, 138.3, 139.5, 145.3, 151.5, 156.9, 194.2; $M^{+.1}$ = 414.

1-(4-chlorophenyl)-3,7,7-trimethyl-4-phenyl-6,7,8,9-tetrahydro-1H-pyrazolo[3,4-b]quinolin-5(4H)-one (4f)

Melting Range: 176-178 ^{o}C; Yield %: 90%;^{1}H NMR (400 MHz; DMSO-d_6;TMS) δ_H: 0.9 (s, 3H,

CH_3), 1.0 (s, 3H, CH_3), 1.9 (s, 3H, CH_3), 2.1-2.3 (d, 4H, CH_2), 5.0 (s, 1H, CH), 6.5 (s, 1H, NH),7.0-8.0 (m, 9H, Ar-H); ^{13}C NMR δC (100 MHz; DMSO-d6): 12.1, 27.3, 28.9, 29.0, 32.5, 42.5, 50.8, 104.3, 111.9, 121.1, 124.5, 127.5, 129.3, 129.5, 129.9, 131.2, 135.6, 137.5, 144.1, 147.5, 148.9, 195.2; M^{+}. = 417, M^{+2}. = 419.

1-(4-fluorophenyl)-3,7,7-trimethyl-4-phenyl-6,7,8,9-tetrahydro-1H-pyrazolo[3,4-b]quinolin-5(4H)-one (4g)

Melting Range: 221-222 ^{o}C; Yield %: 89%; ^{1}H NMR (400 MHz; DMSO-d6;TMS) δ_H: 0.9 (s, 3H, CH_3), 1.0 (s, 3H, CH_3), 1.9 (s, 3H, CH_3), 2.1-2.3 (d, 4H, CH_2), 5.1 (s, 1H, CH), 6.6 (s, 1H, NH),7.0-8.0 (m, 9H, Ar-H); ^{13}C NMR δC (100 MHz; DMSO-d_6): 12.1, 27.3, 28.9, 29.6, 32.5, 35.5, 42.2, 50.8, 104.5, 112.0, 121.9, 125.1, 126.9, 129.3, 129.8, 129.9, 135.6, 137.9, 142.3, 142.5, 148.9, 162.39, 195.2; $M^{+.1}$ = 402.

1-(4-ethylphenyl)-3,7,7-trimethyl-4-phenyl-6,7,8,9-tetrahydro-1H-pyrazolo[3,4-b]quinolin-5(4H)-one (4h)

Melting Range: >220 ^{o}C; Yield %: 90%; ^{1}H NMR (400 MHz; DMSO-d_6;TMS) δ_H: 0.9 (s, 3H, CH_3), 1.0 (s, 3H, CH_3), 1.2 (t, 3H, CH_3), 1.9-2.2 (d, 4H, CH_2), 2.6 (q, 2H, CH_2), 5.0 (s, 1H, CH), 7.0-8.0 (m, 9H, Ar-H), 9.2 (s, 1H, NH),; ^{13}C NMR δC (100 MHz; DMSO-d6): 11.9, 15.0, 19.2, 26.8, 28.9, 31.1, 40.7, 50.9, 104.3, 110.1, 120.8, 123.4, 125.5, 125.8, 126.8, 128.8, 129.5, 129.9, 134.1, 136.2, 138.4, 145.2, 151.7, 194.1; $M^{+.1}$ = 412.

Cytotoxicity assay

The cytotoxicity of SKOV-3 (Human ovarian carcinoma) and PC-3 (Human prostate carcinoma) cells were measured using colorimetric method such as MTT assay (Sigma USA) [13-14]. Cells were seeded at a density of 2×10^5 cells in 100 µL of DMEM cell culture medium and cultured for a period of time 24 h in 96 well sterilized plate prior to addition of the test compounds. Different concentrations of test compounds were added to the cells and incubated for 48 hr. Doxorubicin was used as positive control. All the cells were incubated with 10 % MTT solution for 2 hr at 37 °C. The optical density of the solubilized formazan crystals in DMSO was recorded at 570 nm using multimode reader [15-16].

Molecular Docking

In order to examine the binding interactions of synthesized molecules with the target protein, molecular docking studies were performed using AutoDockTools [Ghanbari et al., 2019]. The 3D structures of active compounds such as 4d and 4g were constructed using Chem3D Ultra 16.0 software. Afterwards, energies of the ligands were minimized with 0.10 RMS gradient and 100 iterations using MOPAC (semi-empirical quantum mechanics). The PDB structure of target protein Human Phosphodiesterase 4B (PDB ID: 1Y2J) with co-crystal ligand 7DB was downloaded and imported to the workspace. The protein structure was optimized and the water molecules were removed. Further, the hetero atoms were removed and geisteiger charges were incorporated to the protein structure. Later the ligands were docked to the processed protein. The output files generate from docking were analysed by using PyMol. Co-crystal ligand 7DB (3,5-dimethyl-1-(3-nitro-phenyl)-1H-pyrazole-4-carboxylic acid ethyl ester) was used as positive control to validate the results. All the docked poses were observed and the best pose was taken. LIGPLOT was used to show the 2D binding interactions of the ligands with target protein [17].

CONCLUSION

In conclusion, we have developed a simple and efficient green protocol for the synthesis of pyrazole conjugated tetrahydroquinoline derivatives using 3-methyl-1-phenyl-1H-pyrazol-5-amine 1, 5,5-dimethylcyclohexane-1,3-dione 2, and benzaldehydes 3 as synthons, utilizing the environmentally friendly property of [DBUH][OAc] as the green reaction medium. Later, the synthesized derivatives examined their anticancer potential against SKOV-3 and PC-3 cells. Among all, compound 4g showed good inhibition activity towards SKOV-3 and PC-3 cells with an IC_{50} value of 8.1 and 9.3 µM, respectively. In additional, insilico studies revealed that the compound 4g exhibited good binding affinity (-8.5 Kcal/mol) towards Human Phosphodiesterase 4B.

Acknowledgement

Authors KK and VAR are very thankful to the authorities of GRIET and IAE for providing research facilities.

Brown, T., 2019. Renewable hydrogen for sustainable ammonia production. *Chemical Engineering Progress*, *115*(8), pp.47-53.

REFERENCES

1. Karthikeyan, C., Malla, R., Ashby, C. R., Amawi, H., Abbott, K. L., Moore, J., Chen, J., Balch, C., Flannery, P. C., Trivedi, P., Lee, C., Faridi, J. S., Pondugula, S. R., and Tiwari, A. K., 2016. Pyrimido[1″,2″:1,5]pyrazolo[3,4-b]quinolines: Novel compounds that reverse ABCG2-mediated resistance in cancer cells. *Cancer Lett*, 2016, *376*, pp. 118–126. DOI: 10.1016/j.canlet.2016.03.030
2. Karnakar, K., Narayana, S. M., Ramesh, K., Satish, G., Jagadeesh, B. N., Nageswar, Y.V.D., 2012. Polyethylene glycol (PEG-400): an efficient and recyclable reaction medium for the synthesis of pyrazolo[3,4-b]quinoline derivatives. *Tetrahedron Letters., 53*, pp. 2897–2903. http://dx.doi.org/10.1016/j.tetlet.2012.03.135
3. Mohamed, L. W., Shaaban, M. A., Zaher, A. F., and Elsahar, A. M., 2019. Synthesis of new pyrazoles and pyrozolo [3,4-b] pyridines as anti-inflammatory agents by inhibition of COX-2 enzyme. *Bioorg. Chem.*, 2019, *83*, pp. 47–54. https://doi.org/10.1016/j.bioorg.2018.10.014
4. Sedlák, D., Wilson, T. A., Tjarks, W., Radomska, H. S., Wang, H., Kolla, J. N., Leśnikowski, Z. J., Špičáková, A., Ali, T., Ishita, K., 2021. Structure–Activity Relationship of para-Carborane Selective Estrogen Receptor β Agonists. *Journal of Medicinal Chemistry., 64*, pp. 9330-9353. https://doi.org/10.1021/acs.jmedchem.1c00555
5. Safaei-Ghomi, J., Sadeghzadeh, R., and Shahbazi-Alavi, H., 2016. A pseudo six-component process for the synthesis of tetrahydrodipyrazolo pyridines using an ionic liquid immobilized on a $FeNi_3$ nanocatalyst. *RSC Adv.*, 2016, *6*, pp. 33676–33685. https://doi.org/10.1039/C6RA02906J
6. Paul, S., and Das, A. R., 2013. PEG-OSO_3H in aqueous reaction medium: synthesis of highly substituted structurally diversified coumarin and uracil fused spirooxindoles. *Tetrahedron Lett., 54*, pp. 1149–1154. https://doi.org/10.1016/j.tetlet.2012.12.079
7. Bhattacharjee, D., Kshiar, B., and Myrboh, B., 2016. L-Proline as an efficient enantioinduction organo-catalyst in the solvent-free synthesis of pyrazolo[3,4-*b*]quinoline derivatives *via* one-pot multi-component reaction. *RSC Adv.*, pp. 95944–95950. https://doi.org/10.1039/C6RA22429F
8. Khurana, J. M., Chaudhary, A., Nand, B., and Lumb, A., 2012. Aqua mediated indium(III) chloride catalyzed synthesis of fused pyrimidines and pyrazoles. *Tetrahedron Lett., 53*, pp. 3018–3022. https://doi.org/10.1016/j.tetlet.2012.04.001
9. Ramesh, V., Purna, P. C. R., Ramachandran, D., and Kalyan, A. C., 2019.One-pot syntheses of 2-

(1h-benzo[d]oxazole-2-yl)-narylbenzamides by self-catalysis. *Eur. Chem. Bull., 8*, pp. 318-321. DOI: http://dx.doi.org/10.17628/ecb.2019.8.318-321

10. Sheldon, R. A., 2001. Catalytic reactions in ionic liquids. *Chem. Commun.*, pp. 2399-2407. https://doi.org/10.1039/B107270F
11. Toda, F., Tanaka, K., 2000. Solvent-free organic synthesis. *Chem. Rev.*, 2000, Vol. 100, p. 1025. https://doi.org/10.1021/cr940089p
12. Luo, Z. Y., Zang, Q. S., Oderaotoshi, Y., Curran, D. P., 2001. Fluorous mixture synthesis: a fluorous-
    tagging strategy for the synthesis and separation of mixtures of organic compounds. *Science*., 2001, *291*, pp. 1766. DOI: 10.1126/science.1057567
13. Temple, C., Rose, J. D., Comber, R.N., and Rener, G.A. 1987. Synthesis of potential anticancer agents: imidazo[4,5-c]pyridines and imidazo[4,5-b]pyridines. *J. Med. Chem,. 30,* pp. 1746. https://doi.org/10.1021/jm00393a011.
14. Mosmann T. 1983. Rapid colorimetric assay for cellular growth and survival: application to proliferation and cytotoxicity assays. *J Immunol Method.s, 65*, pp. 55-63. DOI:10.1016/0022- 1759(83)90303-4.
15. Kumar, R. N., Poornachandra, Y., Nagender, P., Mallareddy, G., Kumar, N. R., Ranjithreddy, P., Kumar, C. G., and Narsaiah, B. 2016. Synthesis of novel trifluoromethyl substituted furo[2,3-b]pyridine and pyrido[3′,2′:4,5]furo[3,2-d]pyrimidine derivatives as potential anticancer agents. *European journal of medicinal chemistry, 108*, pp. 68-78. https://doi.org/10.1016/j.ejmech.2015.11.007.
16. Ghanbari-Ardestani, S., Khojasteh-Band, S., Zaboli, M., Hassani, Z., Mortezavi, M., Mahani, M., Torkzadeh-Mahani, M. 2019. The effect of different percentages of triethanolammonium butyrate ionic liquid on the structure and activity of urate oxidase: Molecular docking, molecular dynamics simulation, and experimental study. *Journal of Molecular Liquids, 292*, pp. 111318. doi 10.1016/j.molliq.2019.111318.
17. Wallace, A. C., Laskowski, R.A., Thornton, J. M. LIGPLOT: a program to generate schematic diagrams of protein-ligand interactions. *Protein engineering, design and selection*, 1995, vol. 8, p. 127–134. doi 10.1093/protein/8.2.127